Drying of a charge-stabilized colloidal suspension *in-situ* monitored by *vertical* small angle X-ray scattering

Sunhyung Kim[1], Kyu Hyun[2], Yun Soo Kim[3,§], Bernd Struth[4],

Christian Clasen[1] and Kyung Hyun Ahn[3,*]

[1]Department of Chemical Engineering, KU Leuven, W. de Croylaan 46, B-3001, Heverlee, Belgium

[2]School of Chemical and Biomolecular Engineering, Pusan National University, Jangjeon-Dong 30, Busan 609-735, Republic of Korea

[3]School of Chemical and Biological Engineering, Institute of Chemical Process, Seoul National University, Seoul 151-744, Republic of Korea

[4]DESY, Notkestrasse 85, D-22607 Hamburg, Germany

*Corresponding Author: ahnnet@snu.ac.kr, +82-2-880-8322

§Current address: Center for Molecular and Engineering Thermodynamics, Department of Chemical and Biomolecular Engineering, University of Delaware, Newark, Delaware 19716, United States

Abstract

We report a first application of *vertical* small angle X-ray scattering to investigate the drying process of a colloidal suspension by overcoming gravity related restrictions. From the observation of the drying behavior of charge-stabilized colloidal silica *in situ*, we find the solidification of the colloidal particles exhibits an initial ordering, followed by a sudden aggregation when they overcome an electrostatic energy barrier. The aggregation can be driven not only by capillary pressure but also by thermal motion of the particles. The dominating contribution is determined by the magnitude of the energy barrier at the transition, which significantly decreases during drying due to an increased ionic strength.

Keywords

Drying, colloidal dispersion, phase behavior, vertical small angle x-ray scattering

1. Introduction

Drying of colloidal dispersions to create thin solid films is a common process for various applications such as photonic crystals, secondary batteries and ceramic films[1, 2]. When a liquid film solidifies during drying, the concentration not only of particles but also of other components increases and the corresponding particle interaction changes over time. As a consequence, the structure of the resulting solid film may be different from expectation derived from the original composition of the suspension[3]. Therefore, understanding the drying process in terms of the phase transition is of importance for controlling the structure and properties of the final film.

In-situ synchrotron X-ray or neutron scattering has proven to be one of the most promising tools in understanding the non-equilibrium phase behavior of colloids[4]. However, conventional synchrotron beams are horizontal to the ground, thus they are not able to pass perpendicular through the colloidal suspension which intrinsically settles in a horizontal plane due to gravity. Because of this limitation, scattering has been applied only for a limited number of cases in drying research; for instance, grazing incidence X-ray scattering[5], or in special applications as spray drying[6], sessile drops[7] or dip coating[8] for which horizontal SAXS can be applied. Recently, a unique rheo-SAXS setup has been developed to allow a synchrotron X-ray beam to pass vertically through the plate/plate geometry of a rheometer[9]. From the viewpoint of drying research, this setup allows a beam passing perpendicular through a liquid film, enabling one to probe the structural change of drying colloidal suspensions *in-situ*.

As solvent evaporates, a colloid film inevitably undergoes a liquid/solid transition, often with complicated and intriguing phenomena such as cracking[10], buckling[11] and formation of optically anisotropic structure[12]. For charge-stabilized suspensions, the liquid/solid transition

is discussed as an initial ordering of non-touching particles, followed by subsequent aggregation, as capillary pressure overcomes the repulsive interaction of adjacent particles[11, 13]. However, a clear understanding how a colloidal dispersion experiences the liquid/solid transition is not fully established yet. This is because the evolution of structure during ordering and aggregation could not be precisely measured in previous studies. In addition, the changes in ionic strength and DLVO potential due to solvent evaporation could not be taken into account, thus the calculation of interparticle force at the transition has been based on assumptions of the actual particle concentration.

In the present study, we report the *in situ* observation of the drying process of charge-stabilized colloidal silica using *vertical* SAXS. From the analysis of the structure factor, we track the volume fraction and the particle interaction with respect to drying time, which enables us to determine the evolution of phase behavior during drying. The liquid/solid transition is described by an initial ordering transition, followed by irreversible aggregation of the particles. The irreversible aggregation into a solid film occurs when the particles overcome the electrostatic energy barrier. We find that the level of the electrostatic energy barrier decreases during drying due to the increasing ionic strength. This lowering of the barrier leads in the current case to a situation where the drying-induced aggregation at which the particles overcome the energy barrier can be driven not only by capillary pressure but eventually also by thermal motion.

2. Materials and experimental method

An aqueous colloidal silica of 30 wt% which is charge-stabilized at pH 9.8 (Ludox HS-30, Aldrich, USA) was used without further treatment. A SAXS study of the silica particle reported a radius r = 8 nm with $\sigma/r = 0.14$ where σ is the width parameter of the Schulz distribution function[8]. The colloidal silica particles have a specific surface area of 220 m^2/g

and a density of 2.37×10^3 kg/m^3. The suspension contains Na^+ and OH^- without surfactant according to supplier. Its zeta potential was measured to be -30 mV by electrophoretic measurement (Zetasizer nano zs, Malvern instruments Ltd, UK).

The *vertical* SAXS experiments were performed at the BW1 beamline at DESY (Hamburg, Germany)[9]. The incoming X-ray beam with a wavelength of 1.26 Å is reflected vertically by a special optics made of diamond and passed through a support frame, a lower plate, the drying suspension and subsequently an upper plate (see Fig. 1a). The support frame and the plates were made of VESPEL (Dupont) which provides sufficiently high transmission for X-rays in the applied energy regime of 9.85 keV [9]. The diameter of the lower and upper plates was 38 mm. The optics and geometry were installed in commercial rheometer (Haake Mars, Thermo scientific, USA) which was specially modified to meet the purpose of vertical SAXS experiment. A sample of 0.5 ml of the colloidal silica is loaded onto the lower plate using a pipette, resulting in a film of a diameter of 20 mm and a corresponding height of 1.6 mm assuming a cylindrical geometry. The suspension wetted moderately well the surface of the lower plate. The contact angle was approximately 70° at the edge of the film outgoing from the known contact angles of DI water on a polyimide[14]. We positioned the X-ray beam (area of 400×400 μm^2) at 5 mm from the center of the drying sample, allowing the drying front which moves inward during drying to pass through the beam position (see Fig. 1b). Temperature was controlled at 20±2°C and a relative humidity of 20±5 % was maintained using nitrogen gas purging the environmental chamber at a flow rate of 3 L/min. *In situ* SAXS images of the drying colloids were detected with a Pilatus 100K detector. The sample to detector distance was set to 2.43 m, covering a q range of 0.08 – 0.70 nm^{-1}, which is analogous to a circular scattering image on the detector of 19.0 mm radius. We captured time averaged images over 10 sec at every 30 sec until the film was dried and the image did not change any more. The data analysis of scattering intensity is based on the assumption that the

vertical cross section of the sample is homogeneous at any particular time of drying. This assumption holds for the sample composition investigated in this study. However, this is not a necessity for more dilute or less stable system, for which the recorded X-ray patterns can be a superposition of scattering patterns corresponding to different structural states formed vertically across the sample thickness during drying. Performing experiments with varying sample thickness also gave reproducible results, further supporting that the structure in the cross section of the film under investigation was homogeneous during drying. Settling of particle during drying can be also a limitation for the measurement of vertical SAXS which results in an inhomogeneous structure in a thickness direction. Peclet number for sedimentation[15] defined by Pe_{sed} = UH/D where U, H, D is sedimentation velocity, film thickness and diffusion coefficient, respectively, gives Pe_{sed} = 0.005 << 1 in this system assuming H = 1 mm. This suggests that the sedimentation on the timescale of the drying studies is not playing a role.

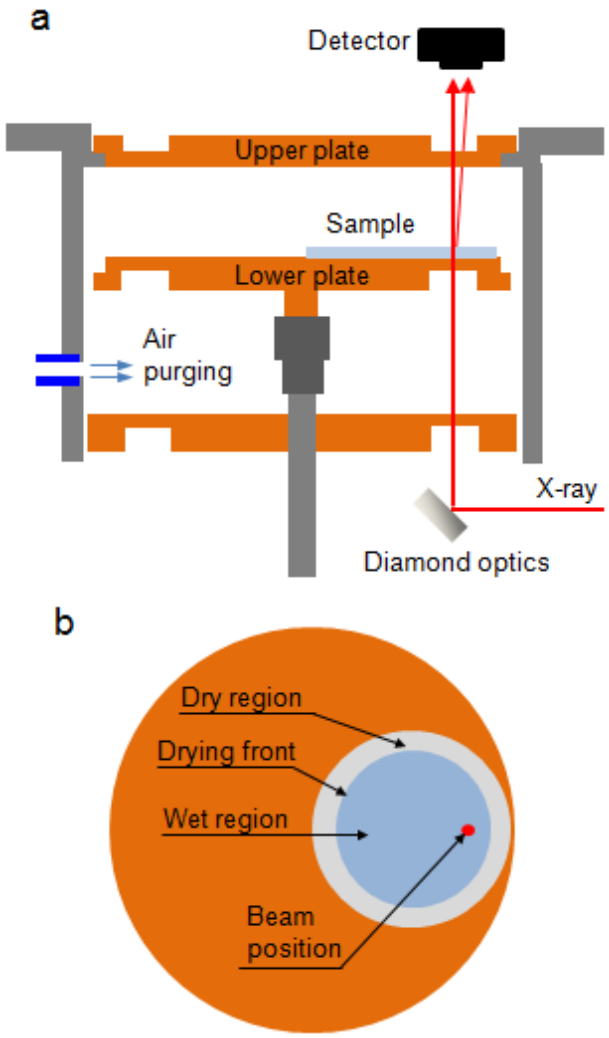

FIG. 1 (color online). Schematics of the drying experiment setup for *vertical* SAXS. (a) The incoming X-ray beam is reflected vertically by a diamond mirror and passes through the plates and the drying sample. (b) Top view of the drying colloidal silica on the lower plate and the position of x-ray beam.

3. Results and discussion

3.1. Interpretation of the scattering intensity

Since the *vertical* SAXS technique is used in the current study for monitoring the drying behavior of colloid film for the first time, the limitations and possible experimental artifacts which may affect the analysis of the scattering intensity were carefully checked. For this, the

form factor of the silica particles obtained with the vertical SAXS setup (BW1) is compared to results determined with a conventional horizontal SAXS (PLS-II 9A U-SAXS beamline, Pohang accelerator laboratory, Korea). To obtain the form factor, we prepared a dilute suspension of the silica particles of 0.05 wt% that was charge screened by the addition of 0.5 M HCl. The SAXS intensities from the two measurement modes, displayed in Fig. 2, show excellent agreement at lower q, but exhibit a deviation in the high q region ($q > 0.5$ nm^{-1}). Fitting the SAXS intensities of the conventional beamline experiment with a theoretical form factor of homogeneous spheres with a Schulz size distribution[4] (solid line in Fig. 2) gives a good agreement at high q range. A slight deviation between experimental and theoretical form factor are observed at low q, which can be attributed to a remaining weakly repulsive particle interaction. The fit of the theoretical form factor yields an average diameter of the particle of r = 7.5 nm with $\sigma/r = 0.145$, which is in good agreement with reported size data[8]. On the other hand, it was not possible to fit the scattering intensity of the vertical SAXS at large q with the same parameters obtained for the conventional SAXS fits. The comparison of the two measurements to the theoretical fit indicates that the systematic deviation of the scattering intensity of the vertical SAXS at higher q ($q > 0.5$ nm^{-1}) is caused by experimental artifacts, and does not originate from the silica particles. This artifact was not observed in a previous work reported for the same setup obtained, however, with a short sample to detector distance[9], and it might thus be attributed to an enhanced noise resulted from the longer distance. We are therefore going to employ the theoretical form factor obtained above for calculations of the structure factor in the following.

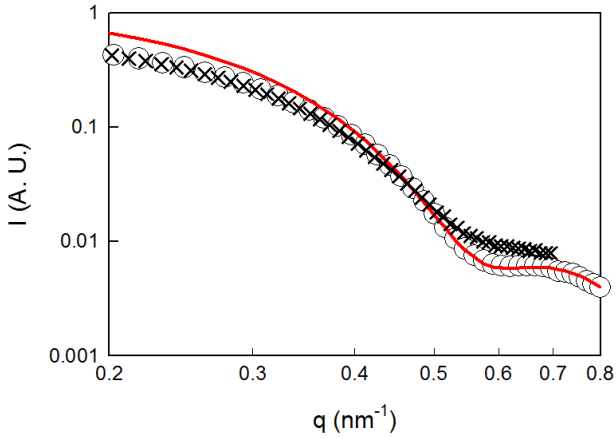

FIG. 2 (color online). The experimental form factor obtained from vertical SAXS (×) and conventional horizontal SAXS (○). They are arbitrarily shifted to fit with the theoretical form factor (solid line).

Scattering images of the colloidal silica suspension are displayed with respect to drying time in Fig 3a. The scattering image at t = 0 min exhibits a bright peak at q = 0.3 – 0.4 nm^{-1}, which is related to the average particle distance controlled by electrostatic repulsion[16]. The position and the intensity of the bright peak change with time, which indicates a structural change during drying. To further interpret the image in Fig 3a, the intensity as a function of q is obtained by averaging over an azimuthal angle of 15° of a scattering image after removing the background scattering.

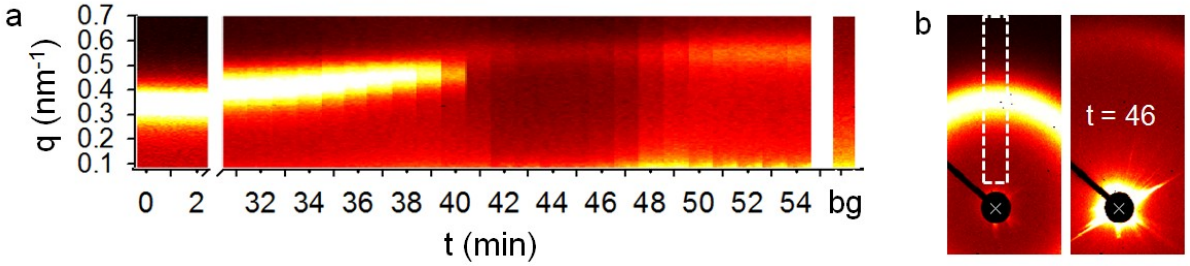

FIG.3 (color online) (a) Scattering images during the drying of charge-stabilized colloidal silica. Images are partly cropped from the original image (see white dashed line in (b)). bg: background measured after removing the dry film. (b) Scattering image obtained from the

detector at t = 0 and 46 min, respectively.

The scattering intensity $I(q)$ in Fig. 4a displays a gradual shift of the position of the peak during drying, indicating a reduction of the average distance between the particles due to the increasing volume fraction of silica particles. In order to relate the position of the peak to the volume fraction, the packing structure needs to be known. Studies on phase behavior of highly charged colloidal particles indicate that strong electrostatic repulsion of monodisperse particles may induce a crystal structure at low particle volume fractions[17]. However, the scattering images from the colloidal silica in this study do not show the signature of a crystal structure (e.g. speckle pattern), likely due to the polydispersity of the particles. Still we assume in the following the suspended particles to be arranged on a primitive cubic lattice, as this has been shown to predict best an average particle distance and volume fraction of colloidal particles when the suspension exhibits a liquid structure[18,19]. The relation between the volume fraction of silica particles and the position of peak can then be expressed by

$$\phi = \frac{r^3}{6\pi^2}\left(q_{peak}\right)^3 \qquad (1)$$

where q_{peak}, ϕ and r are the position of peak intensity, the volume fraction of silica particles, and the radius of the silica particle, respectively. The scattering intensity in Fig 4a yields ϕ = 0.173 at t = 0 min, as displayed in Fig 4b. This is the same as the volume fraction, ϕ = 0.172 calculated from the density of silica within experimental error. ϕ increases gradually during drying but abruptly jumps from ϕ = 0.43 to 0.637 at t = 40 - 42 min. After t = 42 min, the position of peak does not change anymore, and ϕ remains constant at ϕ = 0.637, indicating no further structural development. The final volume fraction in silica film, ϕ = 0.637 is close to, but slightly higher than the random close packed volume fraction (ϕ_{rcp}) of monodisperse

particles, 0.634. A study on the maximum packing density of polydisperse hard-sphere suspension[20] shows that polydispersity increases ϕ_{rcp}, as smaller particles can be incorporated into spaces between larger particles. Since the silica suspension has a polydispersity (i.e. σ/r = 0.145), the slight deviation of the volume fraction from the case of monodisperse particles can be attributed to the polydispersity of the silica particles.

In Fig. 4a, the scattering intensities at low q gradually increase during drying up to t = 40 min which could indicate a partial aggregation of silica particles. However, a comparison of the background intensity to the scattering intensity (inset of Fig. 4a) gives a firm similarity. This suggests that the increased scattering intensity at low q can be interpreted as originating from the background intensity, rather than the aggregation of particles.

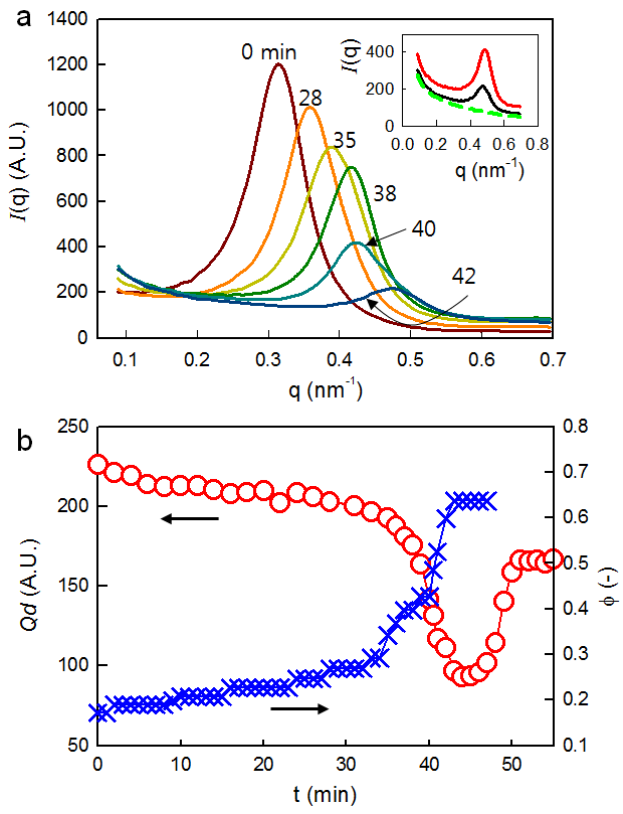

FIG. 4(color online). (a) Scattering intensity with respect to drying time. Inset: t = 54 min, 42 min and background intensity from the top to bottom. The background intensity was arbitrarily shifted to help the comparison of the scattering intensity at t = 42 min. (b)

Scattering power Qd (○), and volume fraction of colloidal silica ϕ (×) with drying time.

The measured scattering intensity *I(q)* is influenced not only by the spatial arrangement of the particles, but also by the evolution of sample thickness during drying. The film thickness, which is not strictly related to the shape of SAXS intensity can be obtained from the scattering invariant, *Q*: the integration of the measured scattering intensity over all scattering vectors[4, 21]. As $I(q)$ in Fig 4a is not scaled by sample thickness, the scattering invariant for a drying film is expressed by[8]

$$Qd = \int_0^\infty I(q)q^2 dq = 2\pi^2 d\left(\rho_p - \rho_m\right)^2 \phi(1-\phi) \qquad (\text{Eq. 2})$$

where d is the film thickness and $(\rho_p - \rho_m)^2$ is the scattering contrast, the square of the difference between the scattering length densities of the particles, ρ_p and of the medium, ρ_m. Qd obtained from the integration of $I(q)$ over q in the range of q = 0.08 – 0.7 nm^{-1} displays initially a gradual decrease during drying that accelerates when approaching t = 35 min (Fig 4b). As ϕ is already obtained from Eq. 1, Eq. 2 only has one unknown assuming a constant $(\rho_p - \rho_m)$ [8]: the film thickness d. Therefore, the evolution of Qd with respect to the drying time in Fig 4b allows us to estimate the evolution of d during drying. With $\rho_p = 1.70\times10^{15}$m^{-2} and $\rho_m = 0.94\times10^{15}$m^{-2} [8], d is calculated to be 1396 μm at t = 0 min and decreases during drying to d = 351 μm at t = 44 min (Fig 5). The calculated d shows an excellent agreement with that obtained from K/ϕ, where K is a constant (K = 230 μm), shown as solid line in Fig 5. Replacing d in the right hand side of Eq. 2 with K/ϕ gives a physical meaning to the constant K as the scattering intensity reduced by the volume fraction of solvent. A good agreement of film thickness d, obtained from Eq.2 and from K/ϕ implies that the number of particles is

conserved in the scattering area during drying, suggesting there is no net flow of the particles during drying. This argument is supported by the visual observation that the solid film does not display the signature of a coffee ring effect at the edge. This can be attributed to a balance of the gradient of osmotic pressure and the drag force exerted on the particles by capillary flow toward the drying front, as extensively discussed by Li et al.[8] . We note that film thickness can be biased in case the sedimentation occurs during drying, as the volume fraction from peak intensity would rise faster in time than the one from the scattering invariant. In our study, this was not observed, supporting the ignorable sedimentation during drying.

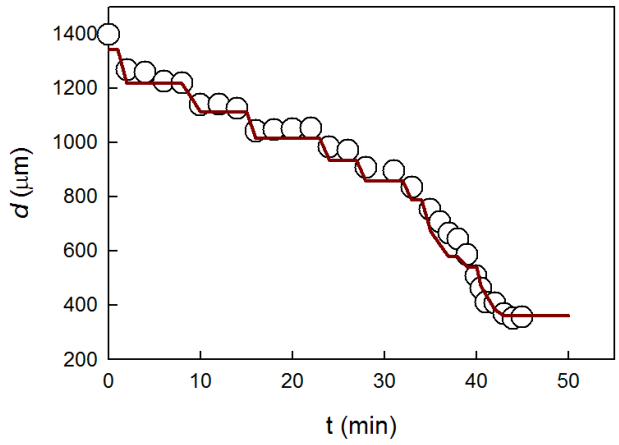

FIG. 5 Thickness of the drying silica film, *d*, obtained from Eq. 2 (open circles) and from K/ϕ (solid line), with a constant K = 230 μm and ϕ as the volume fraction of silica calculated from q_{peak} and Eq. 1.

In Fig 4b, *Qd* shows an upturn from t = 46 min onwards, whereas ϕ does no longer change. This can be attributed to an increase in scattering contrast, resulting from the replacement of water between the particles with air without any further structural change. This argument is supported by the scattering curves shown in the inset of Fig. 4a that display an increase in

$I(q)$ over the whole q range from t = 42 min to t = 54 min without any considerable change in shape. It is worthwhile noting that the scattering image at t = 46 min in Fig. 3b shows an appearance of sharp streaks at low q which stretch radially to higher q, and that this coincides with the emerging bright part at low q ($q < 0.12$ nm^{-1}) in Fig. 3a. Since the silica film displays cracks after drying, the evolution of these images suggests that the cracks form when air intrudes into the pore space of the silica packing and replaces the water, which is consistent to other observations of the onset of cracking in colloid films [10, 13, 22], in particular for particles with low plasticity[23]. It should be noted that the formation of larger, wet cracks as reported by Goehring et al.[13] cannot be probed by the length scale of the SAXS measurements in this report.

3.2. Structural evolution during drying

To understand the drying process of colloidal suspension, it is important to obtain information about not only the volume fraction but also particle interaction with respect to drying time. Scattering techniques have been extensively utilized to understand the particle interaction, for example, not only electrostatic repulsion[16,24,25] in charged colloids, but also steric repulsion[26] or depletion attraction[19,27] in a particle/polymer mixture. A typical procedure to evaluate the particle interaction in a suspension is to obtain the structure factor from the scattering spectra and to compare it to a suitable theoretical structure factor which is derived from particle interaction. Here, we track the evolution of particle interaction during drying in order for a complete understanding of the drying process of the silica suspension. For this, the structure factor is obtained from the SAXS intensity and compared with the Hayter-Penfold model (HP model) which considers electrostatic repulsion in the structure factor[24].

The structure factor of drying silica film is thus obtained from *I(q)* using the following

expression,

$$I(q) = V_{irr}\left(\rho_p - \rho_m\right)^2 d\phi P(q)S(q) \quad ($$

where V_{irr}, $P(q)$ and $S(q)$ are the volume of the sample irradiated by X-rays, form factor and the structure factor, respectively. In this study, $S(q)$ was obtained from $I(q)$ / $P(q)$ by invoking the condition that $S(q) \rightarrow 1$ at large q[8]. The obtained structure factor in Fig 6a exhibits a change in the intensity as well as the position of peak during drying. The peak intensity, $S(q_{peak})$ is displayed with respect to the drying time in Fig 6b, which increases from $S(q_{peak})$ = 2.00 at t = 0 min to $S(q_{peak})$ = 2.73 at t = 37 min. The increase in $S(q_{peak})$ indicates that ordering of silica particles becomes stronger in the suspension during drying. According to the Hansen-Verlet criterion[28], the theoretical value of $S(q_{peak})$ is 2.85 at a disorder/order transition for a mono-disperse hard sphere suspension, but this value is reported to be reduced by the polydispersity[29]. Therefore, $S(q_{peak})$ = 2.73 at t = 37 min may suggest that the silica suspension finally undergoes a disorder/order transition at this time, considering the polydispersity of silica particles in this study. Afterward, we observed that $S(q_{peak})$ abruptly reduces to 1.3 during between t = 38 min and 40 min, suggesting that the particles suddenly lose the ordered structure within this period. This loss of ordering will be discussed in more detail in the next section

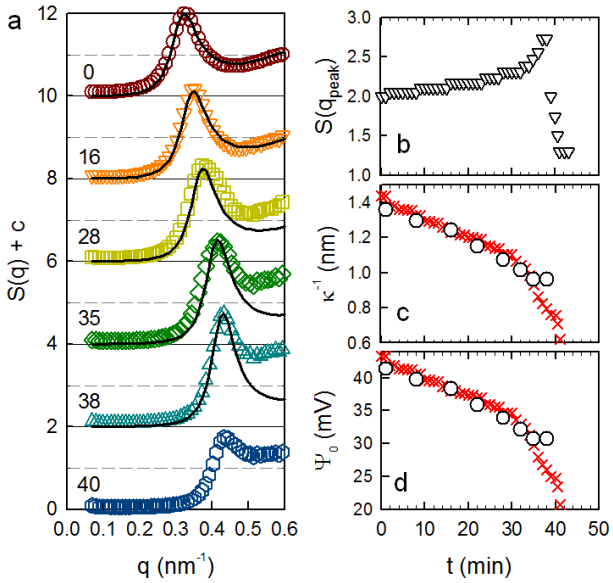

FIG. 6 (color online). Stucture factor, S(q) and the parameters for electrostatic repulsive particle interaction derived from S(q). (a) Structure factor of charged silica with respect to drying time indicated in the graph (unit: min). Solid lines are prediction from the Hayter-Penfold model. Each curve is vertically shifted by a shift factor c: c = 10(0min), 8(16 min), 6(28 min), 4(35 min), 2(38 min), 0(40 min). (b) Peak intensity of S(q) with increasing drying time. (c) Debye lengths and (d) Surface potentials obtained from HP model (○) and derived from volume fraction of particle (×).

To further understand the drying process of colloidal silica from the structure factor, we compare the obtained structure factor with the HP model. The HP model gives a theoretical structure factor by calculating the Ornstein-Zernike equation of an electrostatic potential as a form of direct correlation function in a closed form[24]. The potential (U_e) used in the HP model is given by

$$U_e(h) = 4\pi\varepsilon\varepsilon_0 r^2 \psi_0 \exp\left[-\kappa(h-2r)\right]/h \qquad (1)$$

where, h, ψ_0, and κ are the distance between the particles, the surface potential and the Debye Hückel inverse screening length, respectively. ε and ε_0 are the relative permittivity and the

permittivity of vacuum, respectively. As a result, the comparison of the HP model to S(q) from scattering measurement yields values of the parameters in Eq. 4, κ and ψ_0 . A least square fit of the HP model to the *S*(q) by means of the SASfit software[30], (solid lines, Fig. 6a) gives a nice agreement with the experimental data up to t = 38 min with only a slight discrepancy at high *q*, which can be attributed to experimental artifacts in the vertical SAXS scattering intensity as discussed in the Fig. 1. The disability of HP model to fit the S(q) at t = 40 min may be related to the reduction of $S(q_{peak})$, which suggests that the structure in the suspension at t > 40 min is not dominated by electrostatic repulsion described by HP model anymore. The Debye length κ^{-1} from the HP model (open circle in Fig. 6c) decreases with drying time, which is attributed to an increasing ionic strength during drying. To describe κ^{-1} with drying time, we assume that ionic strength (χ) increases in a proportion with the volume fraction by $\chi \sim \phi/(1-\phi)$ during drying. Since κ^{-1} is proportional to $1/\sqrt{\chi}$ [31], it can be derived from ϕ via

$$\kappa^{-1} = L\sqrt{(1-\phi)/\phi} \qquad (5)$$

where *L* is a constant. As the evolution of ϕ is determined with drying time in Fig 4b, κ^{-1} can be obtained from Eq. 5, which shows a good agreement with κ^{-1} obtained from the HP model (crosses in Fig. 6c) for *L* = 0.663 nm.

The ψ_0 from the HP model decreases during drying similar to κ^{-1} (open circle in Fig. 6d). Here we also describe the behavior of ψ_0 with drying time. In the HP model, ψ_0 is linked to κ^{-1} by[24]

$$\psi_0 = \frac{Z_m}{4\pi\varepsilon\varepsilon_0 r(1+\kappa r)} \quad (6)$$

where Z_m is a surface charge. Calculation of Eq. 6 using κ^{-1} and ψ_0 obtained from the HP model gives $Z_m = 15e$ independent of the drying time, where e is the charge of an electron. The constant Z_m implies that the surface charge is not neutralized upon solvent evaporation. This can be attributed to the fact that the Na^+ ions used to stabilize the colloidal silica in this study are considered indifferent ions which are not adsorbed onto the silica surface, resulting thus in a constant surface charge[31]. The constant $Z_m = 15e$ allows us to calculate ψ_0 from ϕ by inserting Eq. 5 into Eq. 6. Fig. 6d shows a good agreement between ψ_0 calculated from ϕ (cross in Fig. 6d) and ψ_0 obtained from the HP model.

The evolution of ϕ in Fig 4b and κ^{-1} and ψ_0 in Fig. 6c and 6d, respectively, with drying time allows us to understand the complete phase behavior of colloidal silica during drying. For this, we calculate the interaction potential U_e with drying time and subsequently obtain the effective volume fraction (ϕ_{eff}) which includes a contribution of electrostatic repulsion. ϕ_{eff} is given by

$$\phi_{eff} = \phi\left(\frac{r+\delta_{eff}}{r}\right)^3 \quad (7)$$

where δ_{eff} is an effective range of electrostatic repulsion that the approaching particles feel each other. δ_{eff} is calculated from U_e (Eq.3) by[16]

$$\delta_{eff} = \tfrac{1}{2}\int_{2r}^{\infty}\left[1-\exp\left(-U_e/kT\right)\right]dh \quad (8)$$

We show ϕ_{eff} and ϕ with respect to drying time in Fig. 7a and indicate the liquid state (ϕ<0.5), coexistence state ($0.5 < \phi < 0.55$) and solid state ($\phi > 0.55$)[31]. As solvent evaporates, ϕ_{eff}

enters the solid phase regime at t = 37 - 38 min (indicated as τ_1). The entrance of ϕ_{eff} into the solid regime coincides with the peak intensity, reaching $S(q_{peak})$ = 2.73 at t = 37 - 38 min, suggesting that the silica film experiences indeed a disorder/order transition. Since the volume fraction of silica particle is ϕ = 0.4 - 0.42 in this period, the dispersion is still a fluid and this transition at τ_1 should be interpreted as a disorder/order transition induced by the overlap of the effective range of electrostatic repulsion[31].

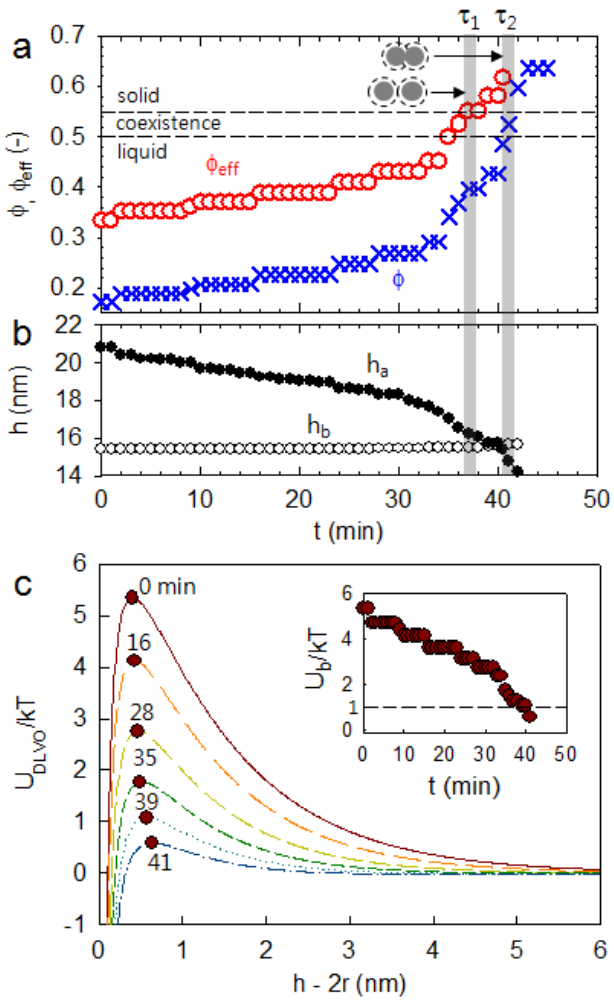

FIG. 7 (color online) The mechanism of the liquid/solid transition. (a) Phase behavior of colloidal silica with drying time. Transitions occurs at times τ_1 and τ_2 where ϕ_{eff} (○)and ϕ(×), respectively, meet the boundary between the coexistence-phase and solid-phase. The first transition at τ_1 occurs as the electrostatic repulsive layers make contact; the second step at τ_2 occurs as the surfaces of the particles make contact, denoting the formation of a virtually

solid film. (b) Average center to center distance of particles, h_a(●), and the position of the energy barrier, h_b(○), with respect to drying time. (c) DLVO potential with respect to surface separation, *h-2r* at different drying time. The energy barrier (○) is indicated at each drying time. (Inset) the magnitude of energy barrier, U_b with respect to drying time.

Subsequently, ϕ enters the solid phase regime at t = 40 - 41 min (indicated as τ_2 in Fig 7a), stepping sharply from 0.45 to 0.637. This indicates that the colloidal silica collapses and experiences a transition to a virtual solid with direct contact of the bare silica particles. Here we note that there is a slight discrepancy between the time at which $S(q_{peak})$ starts to decrease (t = 38 min, Fig. 6b) and ϕ abruptly jumps (t = 40 min, Fig 7a), implying that the sudden aggregation of the silica particles into close packing structure is preceded by a loss of ordered structure. To obtain a clearer view on the aggregation process of particles, we further analyze the particle interaction. We first compare the average particle distance with the position of the energy barrier of the DLVO potential, $U_{DLVO} = U_{vdw} + U_e$. The electrostatic potential U_e is calculated from Eq. 3. The Van der Waals attraction, U_{vdw}, is expressed as[31]

$$U_{vdw}(h) = -\frac{A}{12}\left(\frac{4r^2}{h^2-4r^2} + \frac{4r^2}{h^2} + 2\ln\frac{h^2-4r^2}{4r^2} \right) \quad ($$

where A and h are the Hamaker constant and the average center-to-center distance, respectively. A is assumed to be constant at A = $0.85*10^{-20}$J during drying[31]. From the interparticle potential $U_{DLVO}(h)$ in Fig. 7c, we calculate the center-to-center distance of the particles at the energy barrier, h_b. Comparing h_b with the average particle distance h_a, which is calculated from $q_{peak}h_a = 2\pi$, we find that h_a becomes smaller than h_b right at t = 41 min (Fig. 7b). It has been known that capillary pressure plays a dominating role in the aggregation of particles by letting the particles overcome the repulsive interaction of adjacent particles[11, 13]. Therefore, $h_a < h_b$ at t = 41 min may suggest that this transition is indeed the particles

overcoming the electrostatic repulsive energy barrier by the capillary pressure. We note that the sudden increase in ϕ from 0.45 to 0.637 at τ_2 is not happening simultaneously throughout the sample, but localized close to the drying front, so that indeed the observation of the collapse in the SAXS data coincides with the drying front passing through the beam. This is consistent with the observation of a sudden color change at the drying front[10, 13], implying that the particles abruptly collapse into an aggregated state, forced by the capillary pressure.

It is important to note that the level of the energy barrier, U_b in Fig. 7c decreases with drying time due to the increase in salt concentration. U_b becomes eventually comparable to kT at t = 39 min (inset in Fig. 7c), where the reduction in $S(q_{peak})$ is observed in Fig. 6b. This suggests that also thermal motion of the particles needs to be taken into account as a possible cause for the particles to overcome the energy barrier. It should be noted that the coincidence of the times for overcoming the energy barrier by capillary pressure or by thermal motion is not necessarily related. A more strongly charged suspension than that used in this study would have a higher energy barrier at τ_2, and its final collapse would be caused solely by capillary pressure, which results in a more close-packed ordered state. However, much more interesting is the scenario for the more weakly charge-stabilized suspension, in which the energy barrier would be overcome by the thermal motion before capillary pressure play a role. In this case it could be speculated that the suspension will irreversibly aggregate into a solid network by thermal motion during drying, where capillary pressure plays a minor role in particle aggregation. This would result in a more disordered film with less close packed structure, which can be observed for a drying colloidal gel[32]. This suggests that the arrangement of the particles in a dried film is determined by the level of the energy barrier at the liquid/solid transition, which determines the driving force for aggregation; either capillary pressure or thermal motion – a proposition that requires further investigation. The scope of this work was to demonstrate that the vertical SAXS technique is a useful tool in the analysis

of drying processes.

4. Conclusion

We explore the drying process of charge-stabilized colloidal silica with *vertical* SAXS which enables to overcome gravity-relevant limitations in drying research. The silica suspension experiences an initial disorder/order transition by the overlap of the effective range of electrostatic repulsion among particles, followed by a sudden aggregation into a virtual solid with a direct contact of the bare silica particles when the particles overcome the electrostatic energy barrier. The energy barrier is found to decrease significantly during drying, suggesting that the dominant contribution to overcome the energy barrier, either capillary pressure or thermal motion, is determined by the level of the energy barrier at the liquid/solid transition. This new insight goes beyond the existing drying mechanism of charge-stabilized suspensions which only considers the role of capillary pressure [11, 13]. Moreover, our new approach using vertical SAXS will motivate future researches to understand the fundamental issues in drying of colloids.

Acknowledgement

We thank J Vermant, K Naveen, K Kang, J Dhont, G Naegele and S S Lee for helpful discussions and J W Yoon, J Y Moon, S H Lee and E Stellamanns for support with the experiment. We also thank DESY, Hamburg, for access to the X-ray beam BW1. K H Ahn acknowledges NRF of Korea for funding through No. 20100026139, and K Hyun through No. 2010-0024466. S Kim and C Clasen acknowledge financial support from the ERC Starting Grant No. 203043-NANOFIB. SAXS measurement at beamline 9A, PLS-II were

supported in part by MEST and POSTECH

References

1. Russel, W. B., Mechanics of Drying Colloidal Dispersions: Fluid/solid Transitions, Skinning, Crystallization, Cracking, and Peeling. *AIChE J.* **2011,** 57, 1378-1385.

2. Yin, W.; Lee, D.-H.; Choi, J.; Park, C.; Cho, S., Screen Printing of Silver Nanoparticle Suspension for Metal Interconnects. *Korean J. Chem. Eng.* **2008,** 25, 1358-1361.

3. Kim, S.; Sung, J. H.; Ahn, K. H.; Lee, S. J., Drying of the Silica/PVA Suspension: Effect of Suspension Microstructure. *Langmuir* **2009,** 25, 6155-6161.

4. Zemb, T.; Lindner, P., *Neutron, X-rays and Light. Scattering Methods Applied to Soft Condensed Matter*. North Holland: 2002.

5. Sanyal, M.; Schmidt-Hansberg, B.; Klein, M. F. G.; Munuera, C.; Vorobiev, A.; Colsmann, A.; Scharfer, P.; Lemmer, U.; Schabel, W.; Dosch, H.; Barrena, E., Effect of Photovoltaic Polymer/Fullerene Blend Composition Ratio on Microstructure Evolution during Film Solidification Investigated in Real Time by X-ray Diffraction. *Macromolecules* **2011,** 44, 3795-3800.

6. Sen, D.; Spalla, O.; Taché, O.; Haltebourg, P.; Thill, A., Slow Drying of a Spray of Nanoparticles Dispersion. In Situ SAXS Investigation. *Langmuir* **2007,** 23, 4296-4302.

7. Hu, S.; Rieger, J.; Lai, Y.; Roth, S. V.; Gehrke, R.; Men, Y., In-Situ Observation of Drying Process of a Latex Droplet by Synchrotron Small-Angle X-ray Scattering. *Macromolecules* **2008,** 41, 5073-5076.

8. Li, J.; Cabane, B.; Sztucki, M.; Gummel, J.; Goehring, L., Drying Dip-Coated Colloidal Films. *Langmuir* **2012,** 28, 200-208.

9. Struth, B.; Hyun, K.; Kats, E.; Meins, T.; Walther, M.; Wilhelm, M.; GruÌˆbel, G., Observation of New States of Liquid Crystal 8CB under Nonlinear Shear Conditions as Observed via a Novel and Unique Rheology/Small-Angle X-ray Scattering Combination. *Langmuir* **2011,** 27, 2880-2887.

10. Dufresne, E. R.; Corwin, E. I.; Greenblatt, N. A.; Ashmore, J.; Wang, D. Y.; Dinsmore, A. D.; Cheng, J. X.; Xie, X. S.; Hutchinson, J. W.; Weitz, D. A., Flow and Fracture in Drying Nanoparticle Suspensions. *Phys. Rev. Lett.* **2003,** 91, 224501.

11. Tsapis, N.; Dufresne, E. R.; Sinha, S. S.; Riera, C. S.; Hutchinson, J. W.; Mahadevan, L.; Weitz, D. A., Onset of Buckling in Drying Droplets of Colloidal Suspensions. *Phys. Rev. Lett.* **2005,** 94, 018302.

12. Inasawa, S.; Yamaguchi, Y., Formation of Optically Anisotropic Films from Spherical Colloidal Particles. *Langmuir* **2009,** 25, 11197-11201.

13. Goehring, L.; Clegg, W. J.; Routh, A. F., Solidification and Ordering during Directional Drying of a Colloidal Dispersion. *Langmuir* **2010,** 26, 9269-9275.

14. Matienzo, L. J.; Egitto, F. D., Polymer Oxidation Downstream from Oxygen Microwave Plasmas. *Polym. Degrad. Stabil.* **1992**, 35, 181-192.

15. Cardinal, C. M.; Jung, Y. D.; Ahn, K. H.; Francis, L. F., Drying Regime Maps for Particulate Coatings. *AIChE J*. **2010**, 56, 2769-2780.

16. Qiu, D.; Cosgrove, T.; Howe, A. M.; Dreiss, C. A., A Small-Angle X-ray Scattering Study of the Interactions in Concentrated Silica Colloidal Dispersions. *Langmuir* **2005,** 22, 546-552.

17. Chang, J.; Lesieur, P.; Delsanti, M.; Belloni, L.; Bonnet-Gonnet, C.; Cabane, B., Structural and Thermodynamic Properties of Charged Silica Dispersions. *J. Phys. Chem.* **1995,** 99, 15993-16001.

18. Qiu, D.; Dreiss, C. A.; Cosgrove, T.; Howe, A. M., Small-Angle Neutron Scattering Study of Concentrated Colloidal Dispersions: The Interparticle Interactions between Sterically Stabilized Particles. *Langmuir* **2005,** 21, 9964-9969.

19. Kim, S. Y.; Hall, L. M.; Schweizer, K. S.; Zukoski, C. F., Long Wavelength Concentration Fluctuations and Cage Scale Ordering of Nanoparticles in Concentrated

Polymer Solutions. *Macromolecules* **2010,** 43, 10123-10131.

20. Schaertl, W.; Sillescu, H., Brownian Dynamics of Polydisperse Colloidal Hard Spheres: Equilibrium Structures and Random Close Packings. *J. Stat. Phys.* **1994,** 77, 1007-1025.

21. Glatter, O.; Kratky, O., *Small Angle X-ray Scattering*. Academic press: 1982.

22. Dufresne, E. R.; Stark, D. J.; Greenblatt, N. A.; Cheng, J. X.; Hutchinson, J. W.; Mahadevan, L.; Weitz, D. A., Dynamics of Fracture in Drying Suspensions. *Langmuir* **2006,** 22, 7144-7147.

23. Costa, C. A. R.; Valadares, L. F.; Galembeck, F., Stöber Silica Particle Size Effect on the Hardness and Brittleness of Silica Monoliths. *Colloid. Surface. A* **2007**, 302, 371-376.

24. Hayter, J. B.; Penfold, J., An Analytic Structure Factor for Macroion Solutions. *Mol. Phys*. **1981,** 42, 109-118.

25. Penfold, J.; Ramsay, J. D. F., Studies of Electrical Double-layer Interactions in Concentrated Silica Sols by Small-Angle Neutron Scattering. *J. Chem. Soc., Faraday Trans. 1* **1985,** 81, 117-125.

26. Qiu, D.; Cosgrove, T.; Howe, A. M., Steric Interactions between Physically Adsorbed Polymer-Coated Colloidal Particles: Soft or Hard? *Langmuir* **2006,** 23, 475-481.

27. Ye, X.; Narayanan, T.; Tong, P.; Huang, J. S., Neutron Scattering Study of Depletion Interactions in a Colloid-Polymer Mixture. *Phys. Rev. Lett.* **1996,** 76, 4640.

28. Hansen, J.-P.; Verlet, L., Phase Transitions of the Lennard-Jones System. *Phys. Rev.* **1969,** 184, 151-161.

29. Tata, B. V. R.; Arora, A. K., The Phase Diagram of Charge-Polydisperse Colloids: a Monte Carlo Study. *J. Phys. Condens. Mat.* **1991,** 3, (40), 7983.

30. Kohlbrecher, J.; Bressler, I. *SASfit* 3, 29 June 2007 Laboratory for Neutron Scattering, PSI, Switzerland 2011.

31. Russel, W. B.; Saville, D. A.; Schowalter, W. R., *Colloidal Dispersions*. Cambridge University Press: 1989.

32. Brinker, C. J.; Scherer, G. W., *Sol-gel Science: The Physics and Chemistry of Sol-gel Processing*. Gulf Professional Publishing: 1990.

TOC Graphic

A study of the mechanism of solidification of charge-stabilized colloidal silica during drying, *in situ* monitored by means of a novel technique, *vertical* small angle X-ray scattering (*vertical* SAXS).